SCIENTIFIC REPORTS

OPEN

SUBJECT AREAS:
CLIMATE AND EARTH SYSTEM MODELLING
ATMOSPHERIC DYNAMICS

Received
11 December 2013

Accepted
25 March 2014

Published
10 April 2014

Correspondence and requests for materials should be addressed to K.C.W. (kcwang@bnu.edu.cn)

Sampling Biases in Datasets of Historical Mean Air Temperature over Land

Kaicun Wang

State Key Laboratory of Earth Surface Processes and Resource Ecology, College of Global Change and Earth System Science, Beijing Normal University, Beijing, 100875, China.

Global mean surface air temperature (T_a) has been reported to have risen by 0.74°C over the last 100 years. However, the definition of mean T_a is still a subject of debate. The most defensible definition might be the integral of the continuous temperature measurements over a day (T_{d0}). However, for technological and historical reasons, mean T_a over land have been taken to be the average of the daily maximum and minimum temperature measurements (T_{d1}). All existing principal global temperature analyses over land rely heavily on T_{d1}. Here, I make a first quantitative assessment of the bias in the use of T_{d1} to estimate trends of mean T_a using hourly T_a observations at 5600 globally distributed weather stations from the 1970s to 2013. I find that the use of T_{d1} has a negligible impact on the global mean warming rate. However, the trend of T_{d1} has a substantial bias at regional and local scales, with a root mean square error of over 25% at 5° × 5° grids. Therefore, caution should be taken when using mean T_a datasets based on T_{d1} to examine high resolution details of warming trends.

The measurements of the daily maximum and minimum temperatures (T_{max} and T_{min}) were developed in English-speaking countries once the maximum/minimum thermometers became widely used in approximately 1860[1]. The maximum (or minimum) thermometer is a unique thermometer in that its reading does not change after the air temperature (T_a) reaches T_{max} (or T_{min}). Therefore, T_{max} and T_{min} can be easily measured by checking and resetting the thermometers once a day. The measurements of T_{max} and T_{min} have been accepted globally, and $T_{d1} = (T_{min} + T_{max})/2$ has already become the most common way to calculate mean T_a[2]. In many weather stations, the measurements of T_{max} and T_{min} may be the only data source for historical mean T_a and the only choice for a homogenous century-long analysis of mean T_a[2–4].

Analyses of global mean T_a and its changes are performed operationally by several groups, including the NOAA National Climatic Data Center (NCDC) Global Historical Climatology Network (GHCN)[5–7], the Goddard Institute for Space Studies (GISS)[8], and a joint effort between the Met Office Hadley Center and the University of East Anglia Climate Research Unit (CRUTEM4)[9,10]. All of the global temperature analyses over land performed by the aforementioned groups rely heavily on T_{d1}[11,12]. These century-duration analyses have provided basic datasets for global and regional climate change detection and attribution[13].

However, the use of T_{min} and T_{max} to calculate mean T_a has been criticised because T_{min} is the response of a shallow nocturnal stable boundary layer[12,14], and its variation is sensitive to local land use/land cover[15], surface wind speed and humidity, and downward long-wave radiation from greenhouse gases[16]. T_a reaches T_{min} in the early morning because of long-wave cooling and reaches T_{max} in the early afternoon because of solar short-wave radiation heating (Fig. 1). However, T_a does not change linearly and symmetrically with time (Fig. 1); its diurnal curve depends on the proportion of surface absorbed energy partitioned into sensible and latent heat fluxes (or evapotranspiration)[17], which is determined by the surface incident solar radiation, atmospheric downward long-wave radiation[16], and surface aridity[18]. Therefore, T_{d1} may deviate from real daily mean T_a (i.e., T_{d0}), for both climatology and long-term trends.

In this study, I make a first quantitative assessment of the bias of T_{d1} in quantifying trends of mean T_a using hourly T_a observations collected by the NCDC Integrated Surface Database (ISD)[19], which has provided long-term hourly T_a measurements at approximately 5600 globally distributed weather stations since the 1970s (see Figs. S1 and S2 for detailed information).

Results

The estimation of mean T_a by T_{d1} has two primary sources of bias: (1) T_a has an asymmetric diurnal curve, and (2) T_{d1} collects only two samples of T_a from the early morning to the early afternoon and leaves roughly two thirds of

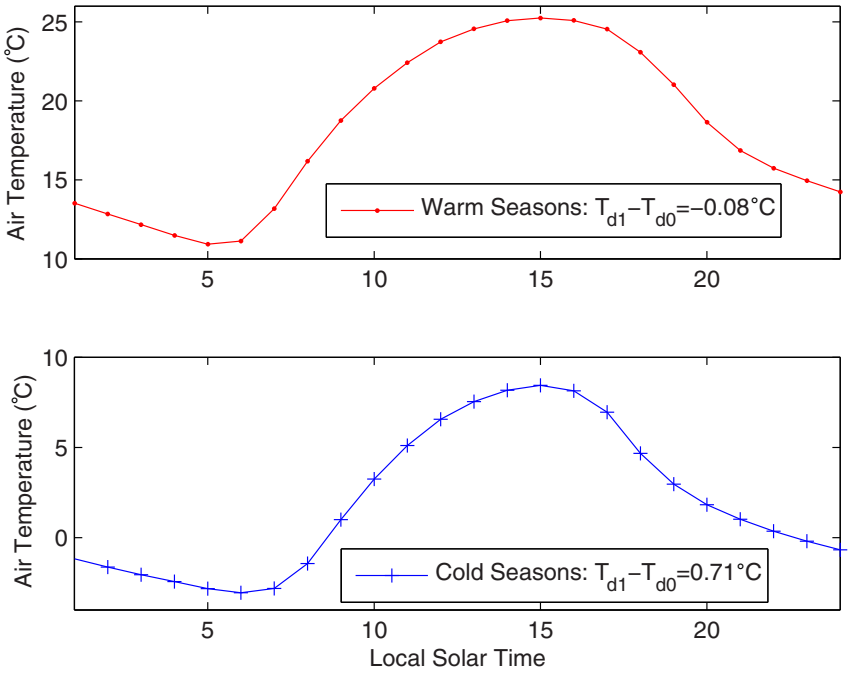

Figure 1 | Multi-year averaged diurnal variation of air temperature (T_a) during the warm seasons (May to October) and cold seasons (November to April) at a station (113.1°W, 37.7°N) in a semi-arid region in the U.S. Because of long-wave cooling, T_a reaches its daily minimum, T_{min}, in the early morning. The temperature reaches its daily maximum T_{max} in the early afternoon because of solar radiation heating. T_a, however, does not change linearly with time. During the cold seasons (Fig. 1b), T_a reaches T_{max} in the early afternoon but decreases quickly afterwards because surfaces receive less incident solar and long-wave radiation. Because of this asymmetric diurnal variation of T_a, $T_{d1} = (T_{max} + T_{min})/2$ is 0.71 °C higher than T_{d0}, integrated from the hourly temperature observations. However, T_{d1} is almost equal to T_{d0} during the warm seasons. The figure was produced using MATLAB.

a day without monitoring. The former introduces systematic bias to T_{d1}, and the later primarily introduces random bias. These two sources of bias are evaluated separately in Figs. 2 and 3, respectively.

The 24-hour T_a from multi-year observations at each station, as shown for example in Fig. 1, are comprised of hourly T_a observations. T_{d0} and T_{d1} are calculated from these composite values. Their differences therefore reflect the impact of the shape of the diurnal variation of T_a on the climatology of T_{d0} and T_{d1}. The mean surface air temperature T_{d1} calculated from T_{max} and T_{min} has a substantially different climatology from that of the real mean surface air temperature T_{d0} (Fig. 2), with a root mean square error of $T_{d1} - T_{d0}$ of approximately 0.3 °C for global land measurements (Table 1). These differences in the climatologies between T_{d1} and T_{d0} are related to the asymmetric diurnal variation of T_a (Fig. 1), which is determined by the surface energy balance. During cold seasons, T_{d1} overestimates the mean surface air temperature T_{d0} almost everywhere. This overestimation is higher in arid or semi-arid regions.

Two factors explain why $T_{d1} - T_{d0}$ is much higher in cold seasons than in warm seasons in arid/semi-arid regions. First, in early morning, a larger fraction of the surface absorbed energy is partitioned into sensible heat flux during the cold seasons[17] because the surfaces are covered by less vegetation and because it is drier in cold seasons than in warm seasons. These conditions result in a faster increase of T_a in the morning under drier conditions because the sensible heat flux directly heats the air above the surface[18]. Second, in the afternoon, the surface long-wave cooling effect is more efficient (Fig. 1) in cold seasons because the compensating effect of atmospheric downward long-wave radiation is lower in the cold seasons due to their lower relative humidity[16]. The combination of these two factors results in higher values of $T_{d1} - T_{d0}$ during the dry cold seasons in arid/semi-arid regions.

T_{d1} samples T_a only twice, during the early morning and the early afternoon, leaving approximately two-thirds of the day unmonitored. The unmonitored times may miss important information about the impact of weather events, such as fronts, on T_a that are important during the cold seasons in the northern high latitudes. The deviation of T_{d1} from T_{d0} may be strong, but it is likely to be randomly distributed. The deviation may be quantified by calculating the standard deviation of the daily $T_{d1} - T_{d0}$. Fig. 3 confirms that the standard deviations of the daily $T_{d1} - T_{d0}$ are higher at the northern high latitudes in the cold seasons and in the global arid/semi-arid regions in both cold and warm seasons. In general, the standard deviations of the daily $T_{d1} - T_{d0}$ in the cold seasons are slightly larger than those in the warm seasons, with a mean value of approximately 0.6 °C (Table 1).

Figs. 2 and 3 show that the deviation of T_{d1} from T_{d0} depends on the asymmetric diurnal variation of T_a, which is related to (a) the surface aridity and vegetation coverage and (b) the timing and frequency of weather events, i.e., front activity. Both aspects may change significantly under climate change conditions[20–22], which may introduce a substantial bias to the trend of the mean surface air temperature through the use of T_{d1}. Fig. 2 implies that the bias of T_{d1} in quantifying the trend of the mean air temperature may be substantial in arid or semi-arid regions if the surface aridity or vegetation coverage changes. I, therefore, further assess the differences in the trends of T_{d1} versus T_{d0} using the NCDC ISD data. Fig. 4 shows the relative biases of the trends, and the statistical results are presented in Table 1. T_{d1} has a negligible impact on the long-term trends of the mean surface air temperature, i.e., the global mean warming rate (Table 1).

The trends calculated from the monthly anomalies of T_{d1}, however, have significant biases relative to T_{d0} at the regional or local scales, with a root mean square error higher than 25% at a $5^\circ \times 5^\circ$ grid scale (Table 1). The spatial coherence of biases in trends of the mean air temperature shown in Fig. 4 is minimal, in contrast with the results in Figs. 2 and 3. Three possible reasons may account for this minimal coherence: (1) the variable changes of the surface conditions occur in both direction and amount at different grids, (2) the measurement bias of the hourly T_a that were used to calculate T_{max}, T_{min},

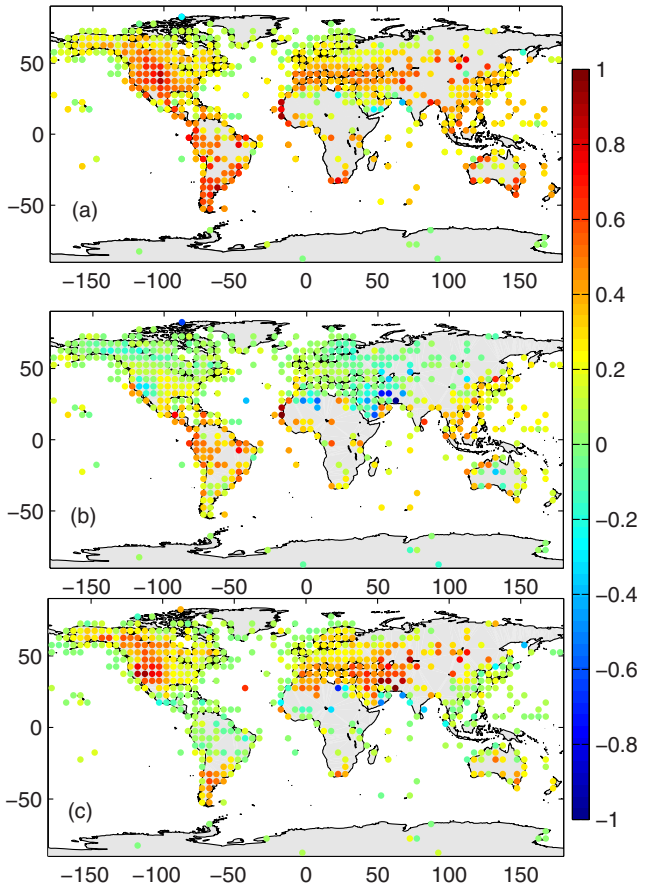

Figure 2 | Multi-year averages of $T_{d1} - T_{d0}$ in units of °C during (a) cold seasons (November to April in the Northern Hemisphere, or May to October in the Southern Hemisphere) and (b) warm seasons (May to October in the Northern Hemisphere, or November to April in the Southern Hemisphere). The differences between cold seasons and warm seasons are shown in panel (c). The 24-hour values of T_a are calculated from the multi-year observations at each station. T_{d0} is integrated from the 24-hour values, and T_{d1} is averaged from the minimum and maximum of the 24-hour values. The climatology difference shown represents $5^\circ \times 5^\circ$ grids, which are integrated from approximately 5600 weather stations. The figure was produced using MATLAB.

T_{d1} and T_{d0}, and (3) the different time periods of data at different grids in Fig. 4, as shown in Fig. S2.

Discussion

In this study, the maximum and minimum hourly T_a measurements are selected to represent T_{max} and T_{min}. However, the response time of the T_{max} and T_{min} thermometer is several minutes. This may introduce some bias to the conclusions of this study. Here, I use the T_a data of five-minute resolution collected by the U.S. Climate Reference Network (USCRN) to demonstrate that it is reliable to use hourly T_a measurements to represent T_{max} and T_{min}.

USCRN has operated since the year 2000 at a few sites and was officially and nationally commissioned by the National Oceanic and Atmospheric Administration (NOAA) in 2004[23,24]. The primary goal of USCRN is to provide long-term high-quality homogeneous observations, in particular, for T_a and precipitation[25]; its temperature system consists of a platinum resistance thermometer and an aspirated radiation shield[24,25]. At each site, the USCRN uses three such thermometers for inter-comparison and quality assurance[25]. These redundant high-level thermometers at each USCRN site guarantee their high-quality continuous observations of T_a (the missing rate of its

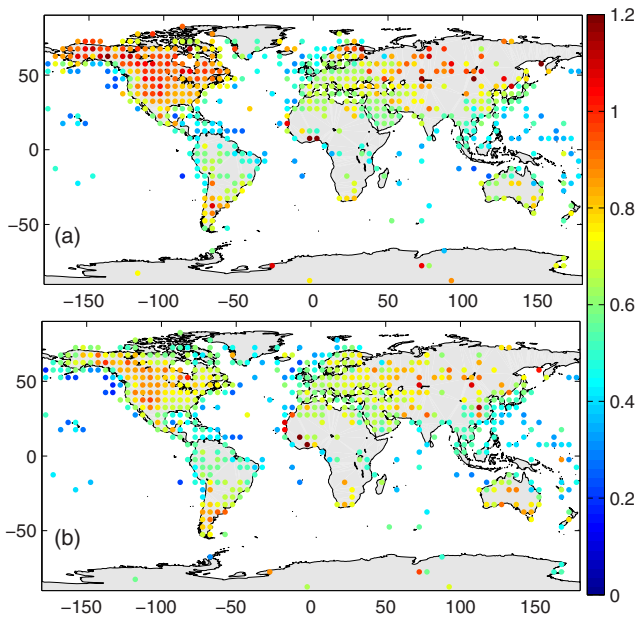

Figure 3 | **Standard deviation of the daily $T_{d1} - T_{d0}$ (units: °C) in (a) cold seasons (November to April in the Northern Hemisphere, or May to October in the Southern Hemisphere), and (b) warm seasons (May to October in the Northern Hemisphere, or November to April in the Southern Hemisphere).** $T_{d1} = (T_{max} + T_{min})/2$ is calculated from the daily maximum temperature (T_{max}) and minimum temperature (T_{min}), and T_{d0} is integrated from hourly values during a day, defined as being from midnight to midnight. The standard deviations at stations are averaged to $5^\circ \times 5^\circ$ grids. The standard deviations between daily T_{d1} and T_{d0} in winter seasons are generally larger than those in warm seasons. Spatially, the standard deviations between the daily T_{d1} and T_{d0} are higher in the northern high latitudes and the global arid/semi-arid regions (Eurasia, North America, South America, Africa, and Australia, see also Fig. S3). The figure was produced using MATLAB.

T_a data is near zero). The data sampling rate of the USCRN thermometers is 5 seconds, and temperature signals averaged over 5-minute intervals are output.

USCRN provides a method for coupling its continuous measurements to the past observations[24,26]. T_{max} and T_{min} can be directly determined from its 5-minute averages[24,26], from which T_{d1} is calculated. We processed all of the data in local solar time. Monthly averages are calculated only if the daily means are available on no less than 24 days in a month and if there are no gaps of four or more consecutive days. The trends of the T_{d0} and T_{d1} are calculated from the monthly anomalies after removing their seasonal cycles. Fig. 5 shows that the biases in the mean values of T_{d1} using the USCRN data are similar to those from the ISD, both in amount and spatial variability. The biases in the relative trend of T_{d1} using the USCRN data are of similar magnitude to those using the ISD data, but with different spatial pattern because the time durations of the two datasets are different. As data availability of the USCRN is temporally and spatially less than that of ISD, the main results in this study are reported using the ISD data.

What are the implications of the biases of T_{d1} and of its trend uncovered in this analysis? It was reported that the warming rate was stronger in the cold-season in semi-arid regions using observations based on T_{d1}[27]. Observations of global mean temperature that are primarily based on T_{d1}, including CRUTEM3, GISS, and NCDC, were used to evaluate T_{d0} from the simulation of the Intergovernmental Panel on Climate Change Fourth Assessment Report (IPCC AR4) climate models. It was found that the model simulations of T_{d0} did not simulate the full extent of the observed

Table 1 | Statistical parameters of the sampling bias of mean surface air temperature $T_{d1} = (T_{max} + T_{min})/2$. The mean temperature T_{d0} is integrated from the hourly values. T_{max} and T_{min} are selected from the hourly values. The data used in the table are hourly observations collected by the NCDC Integrated Surface Database (ISD) over global land. The climatology difference and standard deviation of daily $T_{d1} - T_{d0}$ have units of °C, and the trend of $T_{d1} - T_{d0}$ is in units of °C per decade. The numbers in brackets indicate their relative values

		Average	Median	Root Mean Square
Cold Seasons	Climatology difference of $T_{d1} - T_{d0}$	0.30	0.28	0.36
	Standard deviation of Daily $T_{d1} - T_{d0}$	0.67	0.67	0.70
	Trend of $T_{d1} - T_{d0}$	−0.01 (2.7%)	−0.01 (−1.4%)	0.06 (25.5%)
Warm Seasons	Climatology difference of $T_{d1} - T_{d0}$	0.11	0.09	0.24
	Standard deviation of Daily $T_{d1} - T_{d0}$	0.61	0.63	0.64
	Trend of $T_{d1} - T_{d0}$	0.00 (−1.5%)	−0.00 (−1.0%)	0.06 (27.1%)

winter time warming of T_{d1} at the high-latitude Northern Hemisphere[28]. As shown in Fig. 2, T_{d1} will overestimate the trend of mean T_a if the area gets drier in the arid/semi-arid regions. Observed evidences show it is the case as middle latitude arid or semi-arid regions have been drier in recent decades[29,30]. This partly explains the enhanced warming in semi-arid regions in cold seasons.

Although mean temperature, $T_{d1} = (T_{max} + T_{min})/2$, is perhaps the most common method used to calculate mean air temperature, it is the not the only option. Scandinavian countries developed a special formula to estimate mean T_a[31]. For example, Sweden still uses the Ekholm–Modén formula from 1916, in which the mean T_a is a linear combination of the T_{max}, T_{min}, and measurements of T_a at 6, 12, and 18 h UTC[31]. Another option is to calculate the mean surface air temperature from T_a measurements at 00, 06, 12 and 18 h UTC (T_{d2}), which are recently available through the World Meteorological Organization's (WMO) global telecommunication system[32]. These data have been used in climate-related research[33].

The significant differences in the climatology of T_{d1} and T_{d0} (or T_{d2}), as shown in Fig. 2 (or Fig. S3), preclude switching from the use of T_{d1} to T_{d0} (or T_{d2}) for estimating the long term variability of the mean surface air temperature, although T_{d0} or T_{d2} is already globally available (Figs. 2 and S2). To produce a century-long homogenous dataset of mean T_a, it is essential to continue to use the measurement methods currently used at the weather stations[3,4]. This study indicates that the use of T_{d1} has a negligible impact on the global mean warming rate. However, T_{d1} cannot accurately reflect the impact of

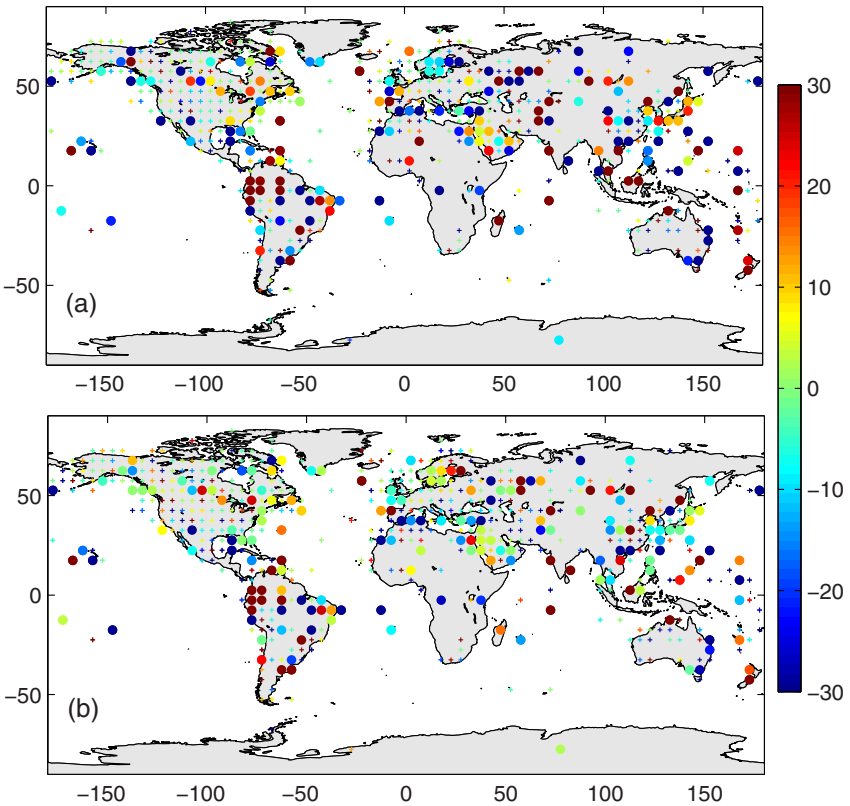

Figure 4 | Bias (%) of the trend of T_{d1} (or the trend of $T_{d1} - T_{d0}$) derived from the global weather observations collected by the NCDC ISD (Integrated Surface Database) and normalised by the trend of T_{d0}: (a) cold seasons (November to April in the Northern Hemisphere, or May to October in the Southern Hemisphere), and (b) warm seasons (May to October in the Northern Hemisphere, or November to April in the Southern Hemisphere). The data shown here are integrated into $5^\circ \times 5^\circ$ grids from approximately 5600 weather stations with different data periods for each station (see Fig. S2 for detailed information). $T_{d1} = (T_{max} + T_{min})/2$ is calculated from the daily maximum temperature (T_{max}) and minimum temperature (T_{min}), and T_{d0} is integrated from the hourly values at the NCDC ISD stations. The dots indicate that the trends of $T_{d1} - T_{d0}$ pass the $\alpha = 0.05$ Student's t-test, and the small pluses indicate that the trends do not pass the confidence test. The positive values indicate that T_{d1} overestimates the long-term trend of the mean surface air temperature. The figure was produced using MATLAB.

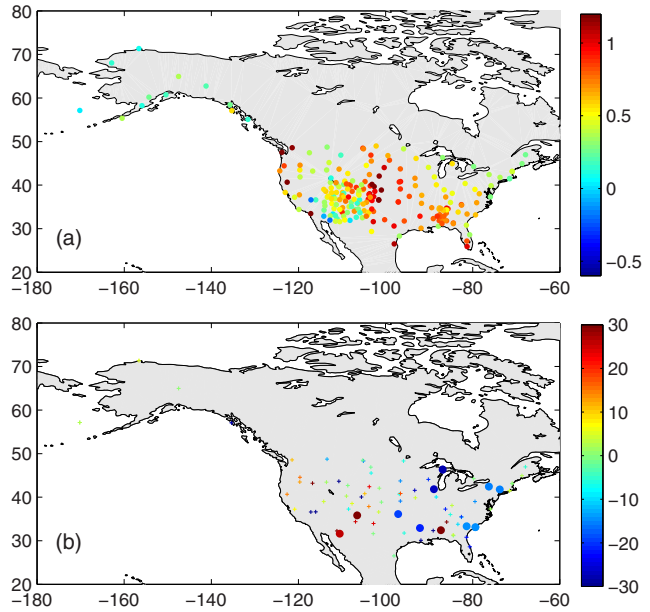

Figure 5 | Multi-year averages of (a) $T_{d1} - T_{d0}$ in units of °C, and (b) the trend of $T_{d1} - T_{d0}$ normalised by the trend of T_{d0} in units of %. The observations of the air temperature at five-minute temporal resolution collected by USCRN from 2004 to 2013 are used here. T_{d0} is integrated from the five-minute values from midnight to midnight, and T_{d1} is averaged from the minimum and maximum of the five-minute values. The dots indicate that the trends of $T_{d1} - T_{d0}$ pass the $\alpha = 0.05$ Student's t-test, and the small pluses indicate that the trends do not pass the confidence test. Each symbol represents a USCRN site. The positive values indicate that T_{d1} overestimates the long-term trend of the mean surface air temperature. The biases are limited to ±30%, avoiding normalisation by near-zero trends. The figure was produced using MATLAB.

the changes in the surface conditions on the variability of T_a. These changing surface conditions cause the diurnal curve of T_a to vary with time, thereby resulting in the deviation of T_{d1} from T_{d0}. Therefore, the trend of T_{d1} has a substantial bias at regional and local scales, with a root mean square error of over 25% for $5^\circ \times 5^\circ$ grids. Careful attention should be paid when using mean surface air temperature T_{d1} on studies regarding the spatial patterns of warming. For such studies, recently available hourly measurements[19] are recommended.

Factors that can introduce inhomogeneity to the mean T_a have been reviewed by Jones et al.[34]. In particular, by assuming that a departure from differently derived mean values are comparable, Bradley and Jones[35] inferred that the monthly temperature values and the hemispherical estimates from different definitions were the same if calculated as anomalies from a selected period. This study confirms this assumption by demonstrating that the global mean trend calculated from the monthly anomalies of T_{d1} is the same as that of T_{d0}. However, the trends calculated from the monthly anomalies of T_{d1} at $5^\circ \times 5^\circ$ grids have a significant error, with a standard deviation of 25%. This large error is caused by the variation of $T_{d1} - T_{d0}$ with changing surface conditions (Fig. 2) as a result of the changing diurnal curve of T_a (Fig. 1).

The use of T_{max} and T_{min} to calculate the mean T_a over land is a result of the fact that many places have used inexpensive instruments that only measure those two temperatures (and could only be checked by an observer once a day) for a long time. T_{min} is more sensitive to changes in land cover[15] and atmospheric downward longwave radiation[12], while the diurnal temperature range ($T_{max} - T_{min}$) is more sensitive to changes in land-atmosphere turbulent fluxes[17], which are driven by variations in the surface incident solar radiation[18] caused by the changes in the clouds and aerosols[36,37]. Observations from T_{max} and T_{min} are therefore very important because of their relationship to climate change impacts and their connection to the global energy balance.

Methods

The hourly observations of T_a over global land collected by the NCDC ISD project[19] were used in this study. The ISD compiles data from over 100 original data sources that archive hundreds of meteorological variables. The ISD has archived 2 billion surface weather observations from over 20,000 stations worldwide from 1900 to the present. Currently, the ISD database is updated with observations from over 11,000 active stations on a daily basis.

The ISD provides consistent and standardised quality control of the global hourly meteorological observations[19]. The ISD contains 54 quality control (QC) algorithms that serve to process each data observation through a series of validity checks, extreme value checks, internal consistency checks, and external continuity checks. Among all of the parameters, temperatures are among the most extensively validated parameters. The ISD data can be freely downloaded from www.ncdc.noaa.gov/oa/climate/isd/index.php.

As of August 2013, there were approximately 5600 stations reporting hourly T_a measurements for more than five years (Fig. S1). The ISD data were reported in UTC time and converted into local solar time for the purpose of my analysis. To obtain the bias and to reduce the impact of missing data, I produced a composite of the 24 hourly values at each site, i.e., all of the observations were averaged into hourly values, and the 24-hour values of the T_a were obtained for each site. T_{min} and T_{max} were selected from the 24-hour values, from which T_{d1} was calculated. T_{d0} was integrated from the 24-hour values. In this study, I split a year into cold seasons (November to April in the Northern Hemisphere, or May to October in the Southern Hemisphere) and warm seasons (May to October in the Northern Hemisphere, or November to April in the Southern Hemisphere). The climatological differences of T_{d1} and T_{d0} were aggregated into a $5^\circ \times 5^\circ$ grid and are shown in Fig. 2. The composite method used here substantially reduces the impact of missing data on the results in Figs. 1 and 2. If there are no missing data, the results shown in Figs. 1 and 2 should be equal to those based on the daily basis, provided that the day is defined as being from midnight to midnight.

The trends shown in Fig. 4 were calculated differently. T_{min} and T_{max} were first selected from the 24-hour observations for each day at every site. The data were regarded as reliable only if the hourly temperatures were available for more than 22 h a day, from which the daily and monthly T_{d0} and T_{d1} were calculated. The monthly values were regarded as reliable only if the daily values were available for more than 15 days a month. The requirement for hourly air temperature measurements is stricter than that for daily values because this study focuses on the difference of T_{d0} and T_{d1}, which is dominated by the diurnal curve of air temperature. The monthly anomalies of T_{d1} and T_{d0} were calculated at each weather station by removing their averaged seasonal cycle. The monthly anomalies were then aggregated into $5^\circ \times 5^\circ$ grid values. The grid averaged-monthly anomalies were regarded as reliable if the data for each month was available at more than 50% of the stations within the grid. The trends of T_{d0} and $T_{d1} - T_{d0}$ calculated from the grid monthly anomalies are presented in Fig. 4 and Table 1. The data duration of T_{d1} and T_{d0} at the $5^\circ \times 5^\circ$ grid can be found in Fig. S2.

The measurements of T_{min} and T_{max} were developed in English-speaking countries where the maximum/minimum thermometers were widely used since approximately 1860[1]. A maximum thermometer is a unique mercury thermometer that functions by having a constriction in the neck close to the bulb. The mercury is forced up through the constriction by the force of expansion as the temperature increases. When there is a decrease in the temperature, the volume of mercury contracts but cannot return to the bulb because of the narrow of the bulb neck. As a result, the column of mercury breaks at the constriction and remains stationary in the tube. The minimum thermometer works similarly, but it does so with steel pin immersed in clear liquid (i.e., ethyl alcohol) in glass.

The measurements of T_{max} and T_{min} can be made by one visit to the weather station a day. Because of its low cost, the measurements of T_{max} and T_{min} have been accepted globally, and $T_{d1} = (T_{min} + T_{max})/2$ has become the most common method to calculate the mean surface temperature. For most weather stations, the measurements using this method may be the only data source for historical temperature.

The weather stations of ISD directly measured T_{max} and T_{min}, in addition to the hourly temperature. The T_{max} and T_{min} temperatures were defined as the highest and lowest temperatures to have occurred during the past 24 hours. However, the T_{max} or T_{min} measurements may depend on the observation schedule, which may be different from country to country. The definition of a day is therefore different, such as from midnight to midnight or from noon to noon. In Europe, T_{min} and T_{max} are usually reported for 12-hour intervals ending at 6 UTC and 18 UTC and are not necessarily the true T_{min} and T_{max} in many regions, especially during the winter months[38]. This discrepancy occurs because 6 UTC is before the climatologically coldest hour sunrise in the winter in some regions (i.e., Europe)[33] and is also partly a result of the synoptic weather variability. This discrepancy introduces a significant error in the estimations of daily T_{max} and T_{min}[33]. The changes of the observation schedules may also introduce inhomogeneity of the climatology of the surface mean air temperature[38]. These problems can be avoided either by maintaining an unchanged observation schedule at a station or by using hourly observations, as I did here.

The bias caused by changes to the observation schedules of T_{min} and T_{max} may be important[15,38], but are not discussed here because the information on observation schedules is not yet publicly available. Two primary sources of bias of T_{d1} are discussed in this study (Figs. 2 and 3). They have physical meanings and may introduce substantial bias to trends of mean surface air temperature T_{d1}. The differences among the trends of T_{d1} and T_{d0} (Fig. 4), which are much less sensitive to the definition of the day, are calculated using the definition of day as midnight to midnight.

1. Austin, J. F. & McConnell, A. James Six F.R. S. Two Hundred Years of the Six's Self-Registering Thermometer. *Notes Rec. R. Soc.* **35**, 49–65, doi:10.2307/531601 (1980).
2. Zeng, X. & Wang, A. What is monthly mean land surface air temperature? *EOS* **93**, 156–156, doi:10.1029/2012eo150006 (2012).
3. Ding, Y. H. *et al*. Detection, causes and projection of climate change over China: An overview of recent progress. *Adv. Atmos. Sci.* **24**, 954–971, doi:10.1007/s00376-007-0954-4 (2007).
4. Ren, G. Y. *et al*. Recent progress in studies of climate change in China. *Adv. Atmos. Sci.* **29**, 958–977, doi:10.1007/s00376-012-1200-2 (2012).
5. Peterson, T. C. & Vose, R. S. An overview of the global historical climatology network temperature database. *Bull. Amer. Meteor. Soc.* **78**, 2837–2849, doi:10.1175/1520-0477(1997)0782837:aootgh>2.0.co;2 (1997).
6. Lawrimore, J. H. *et al*. An overview of the Global Historical Climatology Network monthly mean temperature data set, version 3. *J. Geophys. Res.* **116**, D19121, doi:10.1029/2011jd016187 (2011).
7. Smith, T. M. & Reynolds, R. W. A global merged land-air-sea surface temperature reconstruction based on historical observations (1880–1997). *J. Clim.* **18**, 2021–2036, doi:10.1175/jcli3362.1 (2005).
8. Hansen, J. *et al*. A closer look at United States and global surface temperature change. *J. Geophy. Res.* **106**, 23947–23963, doi:10.1029/2001jd000354 (2001).
9. Mitchell, T. D. & Jones, P. D. An improved method of constructing a database of monthly climate observations and associated high-resolution grids. *Int. J. Climatol.* **25**, 693–712, doi:10.1002/joc.1181 (2005).
10. Jones, P. D. *et al*. Hemispheric and large-scale land-surface air temperature variations: An extensive revision and an update to 2010. *J. Geophys. Res.* **117**, D05127, doi:10.1029/2011jd017139 (2012).
11. Hansen, J., Ruedy, R., Sato, M. & Lo, K. Global surface temperature change. *Rev. Geophys.* **48**, RG4004, doi:10.1029/2010rg000345 (2010).
12. Pielke, R. A., Sr. *et al*. Unresolved issues with the assessment of multidecadal global land surface temperature trends. *J. Geophys. Res.* **112**, D24S08, doi:10.1029/2006jd008229 (2007).
13. Trenberth, K. E. *et al*. in *Climate change 2007: the physical science basis. contribution of working group I to the fourth assessment report of the Intergovernmental Panel on Climate Change* (eds Solomon, S. *et al*.) 236–247 (Cambridge University Press, 2007).
14. McNider, R. T. *et al*. Response and sensitivity of the nocturnal boundary layer over land to added longwave radiative forcing. *J. Geophys. Res.* **117**, D14106, doi:10.1029/2012jd017578 (2012).
15. Misra, V. *et al*. Reconciling the spatial distribution of the surface temperature trends in the Southeastern United States. *J. Clim.* **25**, 3610–3618, doi:10.1175/jcli-d-11-00170.1 (2012).
16. Wang, K. C. & Dickinson, R. E. Global atmospheric downward longwave radiation at the surface from ground-based observations, satellite retrievals and reanalyses. *Rev. Geophys.* **51**, 150–185, doi:10.1002/rog.20009 (2013).
17. Wang, K. C. & Dickinson, R. E. A review of global terrestrial evapotranspiration: Observation, modeling, climatology, and climatic variability. *Rev. Geophys.* **50**, RG2005, doi:10.1029/2011rg000373 (2012).
18. Wang, K. C. & Dickinson, R. E. Contribution of solar radiation to decadal temperature variability over land. *Proc Natl Acad Sci USA* **110**, 14877–14882, doi:10.1073/pnas.1311433110 (2013).
19. Smith, A., Lott, N. & Vose, R. The integrated surface database: recent developments and partnerships. *Bull. Amer. Meteor. Soc.* **92**, 704–708, doi:10.1175/2011bams3015.1 (2011).
20. Zhang, X. *et al*. Enhanced poleward moisture transport and amplified northern high-latitude wetting trend. *Nature Clim. Change* **3**, 47–51, doi:10.1038/nclimate1631 (2013).
21. Berry, G., Jakob, C. & Reeder, M. Recent global trends in atmospheric fronts. *Geophys. Res. Lett.* **38**, L21812, doi:10.1029/2011gl049481 (2011).
22. Held, I. M. & Soden, B. J. Robust responses of the hydrological cycle to global warming. *J. Clim.* **19**, 5686–5699 (2006).
23. Diamond, H. J. *et al*. U.S. Climate Reference Network after One Decade of Operations: Status and Assessment. *Bull. Amer. Meteor. Soc.* **94**, 485–498, doi:10.1175/bams-d-12-00170.1 (2013).
24. Hubbard, K. G., Lin, X., Baker, C. B. & Sun, B. Air temperature comparison between the MMTS and the USCRN temperature systems. *J. Atmos. Oceanic Technol.* **21**, 1590–1597, doi:10.1175/1520-0426(2004)021<1590:atcbtm>2.0.co;2 (2004).
25. Hubbard, K. G., Lin, X. & Baker, C. B. On the USCRN temperature system. *J. Atmos. Oceanic Technol.* **22**, 1095–1101, doi:10.1175/jtech1715.1 (2005).
26. Sun, B. M., Baker, C. B., Karl, T. R. & Gifford, M. D. A comparative study of ASOS and USCRN temperature measurements. *J. Atmos. Oceanic Technol.* **22**, 679–686, doi:10.1175/jtech1752.1 (2005).
27. Huang, J., Guan, X. & Ji, F. Enhanced cold-season warming in semi-arid regions. *Atmos. Chem. Phys.* **12**, 5391–5398, doi:10.5194/acp-12-5391-2012 (2012).
28. Wallace, J. M., Fu, Q., Smoliak, B. V., Lin, P. & Johanson, C. M. Simulated versus observed patterns of warming over the extratropical Northern Hemisphere continents during the cold season. *Proc Natl Acad Sci USA* **109**, 14337–14342, doi:10.1073/pnas.1204875109 (2012).
29. Wang, K. C., Dickinson, R. E. & Liang, S. Global atmospheric evaporative demand over land from 1973 to 2008. *J. Clim.* **25**, 8353–8361, doi:10.1175/jcli-d-11-00492.1 (2012).
30. Dai, A. Increasing drought under global warming in observations and models. *Nature Clim. Change* **3**, 52–58, doi: http://www.nature.com/nclimate/journal/v3/n1/abs/nclimate1633.html#supplementary-information (2013).
31. Ma, Y. & Guttorp, P. Estimating daily mean temperature from synoptic climate observations. *Int. J. Climatol.* **33**, 1264–1269, doi:10.1002/joc.3510 (2013).
32. WMO. Manual on the global telecommunication system. (World Meteorological Organization (WMO), Genva, Switzerland., 2007).
33. van den Besselaar, E. J. M., Klein Tank, A. M. G., van der Schrier, G. & Jones, P. D. Synoptic messages to extend climate data records. *J. Geophys. Res.* **117**, D07101, doi:10.1029/2011jd016687 (2012).
34. Jones, P. D., New, M., Parker, D. E., Martin, S. & Rigor, I. G. Surface air temperature and its changes over the past 150 years. *Rev. Geophys.* **37**, 173–199, doi:10.1029/1999rg900002 (1999).
35. Bradley, R. S. & Jones, P. D. in *Detecting the Climatic Effects of Increasing Carbon Dioxide* (eds MacCracken, M. C. & Luther, F. M.) 29–53 (U.S. Dep. of Energy, 1985).
36. Wang, K. C., Dickinson, R. E. & Liang, S. Clear sky visibility has decreased over land globally from 1973 to 2007. *Science* **323**, 1468–1470, doi:10.1126/science.1167549 (2009).
37. Wang, K. C., Dickinson, R. E., Wild, M. & Liang, S. Atmospheric impacts on climatic variability of surface incident solar radiation. *Atmos. Chem. Phys.* **12**, 9581–9592, doi:10.5194/acp-12-9581-2012 (2012).
38. Vincent, L. A., Milewska, E. J., Hopkinson, R. & Malone, L. Bias in minimum temperature introduced by a redefinition of the climatological day at the Canadian synoptic stations. *J. Appl. Meteor. Climatol.* **48**, 2160–2168, doi:10.1175/2009jamc2191.1 (2009).

Acknowledgments

This study was funded by the National Basic Research Program of China (2012CB955302) and the National Natural Science Foundation of China (41175126 and 91337111). Dr. Robert E. Dickinson provided insight and helpful comments in preparing a draft of this paper, and Dr. Qian Ma processed some data for this study.

Additional information

Supplementary information accompanies this paper at http://www.nature.com/scientificreports

Competing financial interests: The authors declare no competing financial interests.

How to cite this article: Wang, K.C. Sampling Biases in Datasets of Historical Mean Air Temperature over Land. *Sci. Rep.* **4**, 4637; DOI:10.1038/srep04637 (2014).